

# *Ab initio* MO and DFT study of *syn*-sesquinorbornatrienyl dication and its isoelectronic boron analogue†

Ivana Antol, Zoran Glasovac and Mirjana Eckert-Maksić\*

Division of Organic Chemistry and Biochemistry, Rudjer Bošković Institute, P.O.B. 180, HR-10002, Zagreb, Croatia. E-mail: mmaksic@emma.irb.hr; Fax: +385 1 4680 195; Tel: +385 1 4680 197

Received (in Durham, UK) 11th March 2004, Accepted 28th April 2004  
First published as an Advance Article on the web 15th June 2004

The structure of dication **3**, derived by replacement of the CH<sub>2</sub> bridges in *syn*-sesquinorbornatriene (**5**) by the <sup>+</sup>CH groups and its isoelectronic boron analogue **4** were investigated using *ab initio* MP2/6-31G\* and density functional B3LYP/6-31G\* methods. Three energy minima were found in both species, all of them exhibiting strong bis-homoaromatic interaction of the electron deficient bridges with either central or peripheral double bond(s). The calculated <sup>13</sup>C and <sup>11</sup>B chemical shifts support this conclusion.

## Introduction

Cationic norbornenyl compounds have played a pivotal role in developing the chemistry of positively charged reactive intermediates in organic chemistry.<sup>1</sup> Extensive solvolytic,<sup>2</sup> spectroscopic,<sup>3</sup> X-ray<sup>4</sup> and theoretical<sup>5</sup> studies of these species have been reported over the last 50 years with emphasis on evaluating the existence of non-classical bonding. In a recently reported paper we have discussed the nature of homoaromatic interaction in **1** and **2** obtained by fusing two 7-norbornenyl rings and their isoelectronic boron analogue into *syn*-sesquinorbornenyl framework.<sup>6</sup>

It was shown that both species exhibit 4-center-2-electron (4c/2e) bonding instead of the 3-carbon-2-electron (3c/2e) bonding present in their isolated bicyclic subunits.<sup>2–5</sup> This in turn has led to a dramatic change in pyramidalisation of the olefinic carbon atoms and consequently to the change of the characteristic hinge-like bending<sup>7,8</sup> (*i.e.* in an *endo,endo* fashion, thus moving the two ethylene bridges toward each other) of the *syn*-sesquinorbornene framework to the bending in the *exo,exo* fashion (*i.e.* moving two electron deficient bridges toward each other).

Pursuing further our interest in this topic we present here results of an *ab initio* MO and DFT study for structurally related dications **3** and their dibora analogues **4**, which are formally derived by replacement of the CH<sub>2</sub> bridges with the <sup>+</sup>CH (**3**) or BH (**4**) groups in *syn*-sesquinorbornatriene (**5**), respectively.<sup>9</sup>

These species, although not synthetically available as yet, are of considerable interest from theoretical viewpoint, as they provide a unique possibility for exploring participation of the electron deficient centres in either 4c/2e (with central double bond) or 3c/2e (with either central or one of the peripheral double bonds) within the same framework. A question arises which one of them prevails? In order to provide an answer to this question we shall first search for the important stationary points on the potential energy surface of **3** and **4**. Then, electronic and molecular structure of the located stationary points will be analysed and activation barriers for their interconversion will be evaluated. Finally, the carbon and boron

NMR chemical shifts of **3** and **4** will be compared with the previously published NMR parameters for **1** and **2**. In addition, we shall briefly discuss bonding features of model compounds **6** and **7**.

## Computational methods

In performing calculations we made use of the MP2 method,<sup>10</sup> as well as of density functional Becke-3LYP method,<sup>11</sup> in conjunction with the 6-31G\* basis set,<sup>12</sup> within the specified symmetry constraints. Both methods provide a reliable description of the geometry of pyramidalised olefins as shown earlier by us<sup>13</sup> and others.<sup>14</sup> They have also been frequently used in studying nonclassical structures.<sup>15</sup> Since all of the species considered here are expected to be of nonclassical nature their relative stabilities are expected to be well represented due to cancellation of errors inherent in the approximate nature of the methods applied. All of the stationary points have been positively identified, for minimum energy with no imaginary frequencies and for the transition states with one imaginary frequency. For anharmonicity correction, the calculated ZPV energies were scaled using the following scaling factors:<sup>16</sup> 0.9670 and 0.9806 for the MP2 and B3LYP, respectively. Intrinsic reaction coordinate (IRC) analysis<sup>17</sup> was carried out for each transition state to make sure that it is the transition structure connecting the desired reactants and products.

The <sup>13</sup>C NMR and <sup>11</sup>B NMR chemical shifts were computed by GIAO/B3LYP/6-311+G\*\* method<sup>18</sup> employing MP2 and B3LYP geometries. The <sup>13</sup>C NMR chemical shifts are referenced relative to TMS. The <sup>11</sup>B chemical shifts were computed using B<sub>2</sub>H<sub>6</sub> as reference and then scaled to BF<sub>3</sub>/Et<sub>2</sub>O (δ(B<sub>2</sub>H<sub>6</sub>) = 16.6 vs. BF<sub>3</sub>/Et<sub>2</sub>O). Atomic charges were obtained by using the mixed electron density partitioning based on symmetric Löwdin's orthogonalisation.<sup>19</sup> All molecular pictures and visualisation of orbitals were constructed with MOLDEN.<sup>20</sup>

All calculations were carried out with the Gaussian 98<sup>21</sup> or GAMESS-US<sup>22</sup> programs implemented on Linux-based Athlon MP PC's or cluster of Pentium III and Athlon MP PC's at the Rudjer Bošković Institute.

## Results and discussion

The PES of **3** and **4** were scanned with B3LYP/6-31G\* and the relevant stationary points, *i.e.* for the interconversion that

† Electronic supplementary information (ESI) available: bond distances and bond angles of structures **6a**, **6c**, **7a** and **7c** calculated at the MP2/6-31+G\* and B3LYP/6-31G\* levels of theory (Table S1). See <http://www.rsc.org/suppdata/nj/b4/b403802a/>

takes place between the energy minima were located. In each case, three energy minima designated hereafter with letters “a”, “b” and “c” and the transition state structures for bridge flipping between “a” and “b” and “b” and “c”, respectively were identified. We were not able to locate the TS structure for inter-conversion between “a” and “c”. The structure located with SCAN option had two imaginary frequencies ( $-363.4\text{ cm}^{-1}$  and  $-297.7\text{ cm}^{-1}$  for **4** and  $-471.2\text{ cm}^{-1}$  and  $-392.1\text{ cm}^{-1}$  for **3**), each of them following the reaction path for bridge-flipping in one of the bicyclic subunits. The relative energies of the critical points for **3** and **4** are shown in Figs. 1 and 3. In the next step, structures of the energy minima were re-optimised at the MP2 level. The calculated energies are summarised in Table 1, while the selected bond distances and angles are listed in Table 2. Also included in Table 2 are out-of-plane angles of the central ( $\phi$ ) and the peripheral double bond ( $\tau_1$  and  $\tau_2$ ), as well as the tilting angles  $\alpha$  and  $\beta$ .<sup>23</sup> The positive values of the out-of-plane angle are used to describe structures in which the substituents at the double bonds are oriented toward the *endo* site of molecule, and the negative values to the structures in which the substituents at the double bond are oriented toward the *exo* site of the molecule.<sup>23–27</sup> The tilting angles describe the angles between the plane containing electron-deficient bridge, C(3)–X(11)–C(4)/C(5)–X(12)–C(6)), and the  $\text{C}_b\text{C}=\text{CC}_b$  plane, where  $\text{C}_b$  stands for the bridged carbon atoms.

The MP2 optimised structures of the resulted energy minima are shown schematically in Scheme 2. As no substantial difference between geometries computed with B3LYP and MP2 were observed, we shall discuss only MP2 data unless noted otherwise. The relative energies also show good overall agreement between the two methods (Table 1).

### Structure and energetics of dication 3

For dication **3** the three minima, **3a**–**3c** were located on the PES, with the structure **3a** being the most stable at both levels of theory (Fig. 1). As seen in Scheme 2 each of the cationic centres in the structures **3a** and **3b** participates in a 3c/2e bond giving rise to a sandwiched bis-homoaromatic dication,<sup>28,29</sup> whereas dication **3c** is a 4c/2e species. The structure **3b** was found to be less stable by *ca.* 11 kcal mol<sup>−1</sup>, while structure **3c** lies *ca.* 40 kcal mol<sup>−1</sup> higher in energy than **3a** (Fig. 1). We also note that the calculations predict by  $\sim 6\text{ kcal mol}^{-1}$  lower barrier for bridge flipping between structures **3a** and **3b** than between structures **3b** and **3c**. Furthermore, the transition structure **TS3bc** lies  $\sim 17\text{ kcal mol}^{-1}$  (B3LYP level) higher in

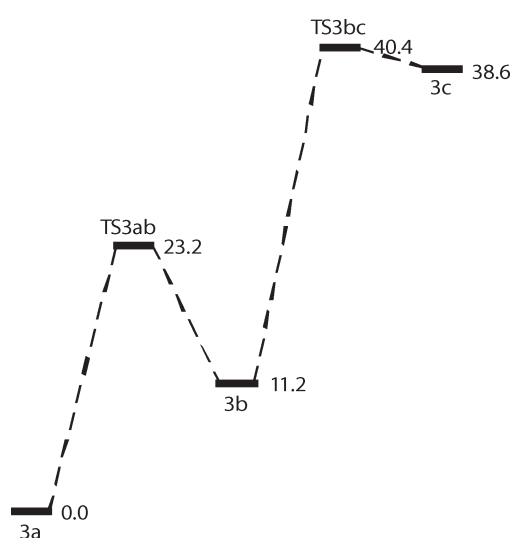


Fig. 1 Schematic energy diagram of the **3a**–**3c** system computed at the B3LYP level. Relative energies are given in kcal mol<sup>−1</sup>.

Table 1 Total energies, vibrational zero point energies and characterisation of stationary points for the different species. Parameters are collected at the MP2/6-31G\* and B3LYP/6-31G\* levels

Compound	$E_{\text{tot}}/\text{a.u.}^a$	Z.P.V.E./a.u. <sup>b</sup>	$E_{\text{rel}}/\text{kcal mol}^{-1}$
MP2/6-31G*			
<b>3a</b>	−460.80947	0.17850	0.0
<b>3b</b>	−460.79123	0.17744	11.5
<b>3c</b>	−460.74127	0.17493	42.8
<b>4a</b>	−435.05187	0.17111	1.9
<b>4b</b>	−435.05489	0.17070	0.0
<b>4c</b>	−435.03446	0.16950	12.8
<b>5</b>	−462.61638	0.20117	—
<b>6c</b>	−462.99267	0.21446	0.0
<b>6p</b>	−462.97337	0.21459	12.1
<b>7c</b>	−450.03216	0.21052	0.0
<b>7p</b>	−450.02924	0.21081	1.83
<b>8</b>	−269.58398	0.11519	—
<b>9</b>	−256.64293	0.11128	—
B3LYP/6-31G*			
<b>3a</b>	−462.29355	0.17897	0.0
<b>3b</b>	−462.27571	0.17795	11.2
<b>3c</b>	−462.23209	0.17566	38.6
<b>4a</b>	−436.51404	0.17117	2.0
<b>4b</b>	−436.51720	0.17089	0.0
<b>4c</b>	−436.50007	0.16986	10.8
<b>5</b>	−464.15549	0.20165	—
<b>6c</b>	−464.53914	0.21446	0.0
<b>6p</b>	−464.51955	0.21451	12.3
<b>7c</b>	−451.56685	0.21038	0.0
<b>7p</b>	−451.56376	0.21053	1.9
<b>8</b>	−270.47841	0.11541	—
<b>9</b>	−257.52748	0.11130	—

<sup>a</sup> corrected for Z.P.V.E. <sup>b</sup> scaled by factor 0.9670 and 0.9806 for MP2 and B3LYP calculations, respectively

energy than **TS3ab**. It is also worth mentioning that the calculated barrier to bridge flipping between **3a** and **3b** is in good accord with experimental estimate for the same process in 7-norbornadiene being 19.6 kcal mol<sup>−1</sup>.<sup>2e</sup>

Evidently, the resulting stabilisation ordering of the located structures represents a balance between the two opposing effects: (a) the charge–charge repulsion which tends to separate the C(11) and C(12) atoms as much as possible and (b) a tendency of the cationic centres to remain planar in order to maximize the overlap between the empty 2p<sub>C</sub>-orbitals with the double filled orbital of either the central or of the peripheral double bond.<sup>30</sup> For instance, it is reasonable to conclude that Coulombic charge repulsion between proximate cationic centres in **3c** (2.8 Å) overrides the stabilization effect gained through 4c/2e bonding, pushing this structure to the highest energy. On the other hand, the reason for the resulting ordering of the structures **3a** and **3b** is less evident. Firstly, separation of the cationic centres in these two structures is large, being relatively close at the same time (4.77 Å and 4.56 Å in **3a** and **3b**, respectively), indicating that destabilisation due to their repulsion should be weak. Secondly, stabilisation gained through bis-homoaromatic interaction in **3b** is expected to be stronger than in **3a** due to involvement of the central double bond in one of the bicyclic fragments. Namely, the difference between the orbital energies of the central and peripheral double bonds<sup>30</sup> gives rise to the expectation that the cationic centre will interact more effectively with the former.<sup>31</sup> The additional support for this proposition is obtained by considering the structure of hypothetical model monocation **6** (Scheme 1). For this cation our calculations predict two energy minima, **6c** and **6p** (Scheme 3), within both computational approaches, with the 3c/2e bond localized over the C(1)–C(2)–C(11) triangle being more stable by  $\sim 12\text{ kcal mol}^{-1}$ . Their MP2 structures

**Table 2** Selected structural parameters of boron compounds **3** and **4** calculated at the MP2/6-31G\* and B3LYP/6-31G\* levels of theory<sup>a</sup>

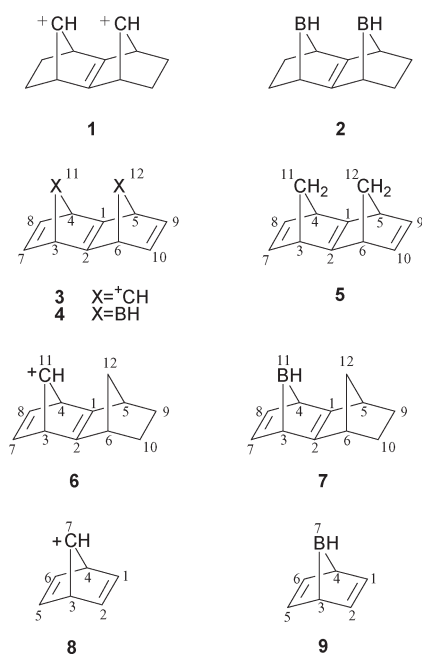
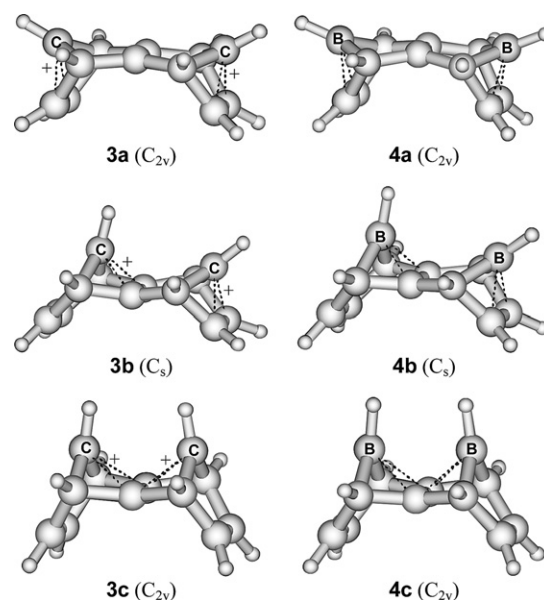
Bond or angle	MP2/6-31G*						B3LYP/6-31G*									
	Compound															
	3a	3b	3c	4a	4b	4c	3a	TS3ab	3b	TS3bc	3c	4a	TS4ab	4b	TS4bc	4c
C(1)–C(2)	1.348	1.407	1.433	1.356	1.398	1.419	1.335	1.360	1.401	1.418	1.419	1.343	1.351	1.388	1.403	1.407
C(2)–C(3)	1.487	1.493	1.545	1.489	1.482	1.508	1.496	1.524	1.502	1.530	1.555	1.498	1.519	1.490	1.495	1.518
C(3)–C(7)	1.503	1.504	1.510	1.492	1.500	1.508	1.512	1.538	1.514	1.517	1.553	1.502	1.538	1.510	1.511	1.520
C(7)–C(8)	1.401	1.342	1.350	1.394	1.347	1.348	1.396	1.352	1.333	1.342	1.341	1.385	1.347	1.338	1.339	1.339
C(3)–X(11)	1.567	1.537	1.488	1.638	1.640	1.607	1.540	1.504	1.538	1.509	1.494	1.649	1.607	1.643	1.633	1.611
C(1)–X(11)	2.388	1.705	1.917	2.498	1.743	1.946	2.397	2.132	1.728	1.858	1.956	2.499	2.260	1.764	1.808	1.973
C(7)–X(11)	1.709	2.419	2.363	1.760	2.517	2.463	1.726	2.242	2.427	2.389	2.370	1.784	2.284	2.521	2.500	2.464
C(2)–C(6)	1.487	1.495	1.545	1.489	1.491	1.508	1.496	1.497	1.505	1.550	1.555	1.498	1.498	1.501	1.529	1.518
C(6)–C(10)	1.503	1.494	1.510	1.492	1.485	1.508	1.512	1.510	1.503	1.543	1.553	1.502	1.501	1.495	1.531	1.520
C(9)–C(10)	1.401	1.403	1.350	1.394	1.394	1.348	1.396	1.396	1.398	1.344	1.341	1.385	1.385	1.385	1.344	1.339
C(6)–X(12)	1.567	1.536	1.488	1.638	1.638	1.607	1.540	1.541	1.537	1.490	1.494	1.649	1.642	1.639	1.607	1.611
C(1)–X(12)	2.388	2.426	1.917	2.498	2.517	1.946	2.397	2.412	2.433	2.147	1.956	2.499	2.504	2.518	2.256	1.973
C(9)–X(12)	1.709	1.724	2.363	1.760	1.773	2.463	1.726	1.734	1.741	2.299	2.370	1.784	1.785	1.797	2.343	2.464
C(1)–C(2)–C(3)	110.5	109.1	107.4	111.4	110.7	109.5	110.6	108.6	109.0	108.1	107.5	111.6	110.0	110.8	110.5	109.5
C(2)–C(3)–C(7)	115.8	114.4	106.1	113.8	113.1	108.6	115.8	112.3	114.6	109.1	106.6	113.9	111.0	113.4	112.0	109.2
C(2)–C(3)–X(11)	104.3	68.5	78.4	106.0	67.7	77.2	104.3	89.5	69.2	75.4	79.8	105.5	92.5	68.3	70.4	78.1
C(3)–X(11)–C(4)	102.2	101.7	104.8	96.5	96.4	97.8	101.7	101.8	101.3	103.6	104.0	96.4	96.1	96.2	97.2	97.5
C(1)–C(2)–C(6)	110.5	109.2	107.4	111.4	110.6	109.5	110.6	110.2	109.2	107.2	107.5	111.6	111.5	110.7	108.8	109.5
C(2)–C(6)–C(10)	115.8	112.8	106.1	113.8	112.4	108.6	115.8	114.0	113.0	106.4	106.6	113.9	113.2	112.4	108.3	109.2
C(2)–C(6)–X(12)	104.3	106.4	78.4	106.0	107.0	77.2	104.3	105.1	106.2	89.8	79.8	105.5	105.7	106.5	92.0	78.1
C(6)–X(12)–C(5)	102.2	102.3	104.8	96.5	96.7	97.8	101.7	102.0	102.1	103.1	104.0	96.4	96.6	96.7	96.1	97.5
$\alpha$	152.3	79.1	93.6	152.2	79.2	92.8	151.7	113.6	80.2	89.2	95.8	150.8	118.4	80.3	83.3	94.2
$\alpha_1$	152.3	155.4	93.6	152.2	153.3	92.8	151.7	153.5	154.4	112.6	95.8	150.8	151.6	151.9	115.7	94.2
$\beta$	79.1	154.4	151.6	80.1	154.0	147.5	79.8	123.9	153.3	151.9	148.7	81.3	119.1	152.4	151.3	145.2
$\beta_1$	79.1	80.8	151.6	80.1	81.3	147.5	79.8	80.6	81.5	132.7	148.7	81.3	81.4	82.6	125.8	145.2
$\phi$	12.2	–19.3	–14.9	21.0	–11.9	–12.6	9.8	–2.2	–18.3	–14.5	–13.5	17.6	10.1	–10.6	–14.7	–12.9
$\tau$	–23.3	3.5	4.2	–17.8	6.9	7.5	–22.8	–3.9	2.8	4.2	3.8	–17.1	–1.4	5.9	6.3	5.7
$\tau_1$	–23.3	–21.9	4.2	–17.8	–16.8	7.5	–22.8	–22.0	–21.5	0.2	3.8	–17.1	–16.7	–16.2	1.8	5.7

<sup>a</sup> All distances are in Å and angles in deg; the numbering scheme is shown on Scheme 1.

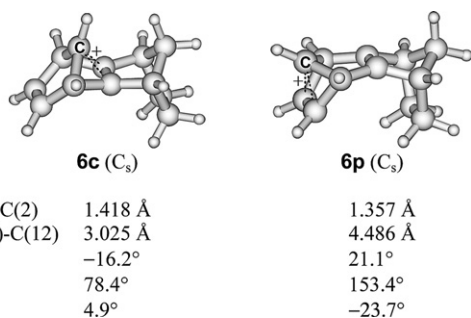
and the key bond distances and bond angles for the unsaturated ring are shown in Scheme 3.

This result unequivocally shows that interaction with the <sup>+</sup>CH bridges with the central double bond in **3b** indeed contributes more to the stability of the cation than interaction of the peripheral double bond, but the original question remains. Why is dication **3a** more stable than **3b**? The answer is offered by comparison of the Löwdin atomic charges in these two

structures (Table 3). It shows that the large fraction of the positive charge of the C(11) and C(12) atoms is shifted to the hydrogen atoms of the <sup>+</sup>CH groups.<sup>32,33</sup> Since the hydrogen atoms are considerably closer in **3b** than in **3a** (3.9 Å vs. 6.5 Å at the MP2 level) it is obvious that the total Coulombic repulsion in **3b** will be significantly higher than in **3a**. This in turn implies that electrostatic interactions play a decisive role in determining relative stabilities of structures **3a–3c**.

**Scheme 1****Scheme 2** Representation of the MP2/6-31G\* geometries of energetic minima of **3** and **4**.





**Scheme 3** MP2 calculated structures and selected structural parameters of structures **6c** and **6p**. Letters **c** and **p** stand for the 3c/2e bonding with the central (**6c**) and the peripheral (**6p**) double bond. More complete compilation of the calculated bond distances and bond angles is given in Table SI of supplemented material†.

Bis-homoaromatic nature of structures **3a–3c** is clearly reflected in the calculated geometries (Table 2) and charge distribution (Table 3) in each of the ions. For instance, in the MP2 optimised structure of the most stable form **3a** the cationic centres are strongly inclined toward the peripheral double bonds; the C(7)–C(11)/C(8)–C(11) and C(9)–C(12)/C(10)–C(12) distances are by 0.679 Å shorter than the C(1)–C(11)/C(2)–C(11) and C(1)–C(12)/C(2)–C(12) distances (2.388 Å). In other words the tilting angle  $\beta$  is by 73.2° smaller than  $\alpha$  (79.1°). The terminal double bond C(7)=C(8) and C(9)=C(10) distances are elongated by 0.058 Å relative to the neutral molecule (1.343 Å), while the central double bond (1.348 Å) retains approximately the same length as in **5** (1.360 Å). Another characteristic feature concerns displacement of the olefinic hydrogen atoms toward one-centre bridges. The computed out-of-plane angle is –23.3° that is only marginally larger than in the 7-norbornadienyl cation (**8**) (–22.7°) calculated at the same level of theory. Geometry of structure **3c** is very similar to that of *syn*-7,7'-sesquinorbornenyl dication (**1**) with the <sup>+</sup>CH groups tilted toward the central double bond bridge.<sup>6</sup> It is interesting to note that the tilting angles  $\alpha$  (in **3c**) are smaller by 3.6° than in dication **1**.<sup>6</sup> This is in accordance with the trend observed previously on comparing 7-norbornenyl with 7-norbornadienyl cation (**8**) (81.4° vs. 78.4°). It is also interesting to note that the degree of pyramidalisation of the C(1) and C(2) atoms of **3c** as measured by the out of plane angle  $\phi$ , is lower than that of **1** (17.9° vs. 14.9° at the MP2 level). This is most likely due to the different ring strain of the 7-norbornenyl and 7-norbornadienyl ring system.

**Table 3** Löwdin's formal charges of **3**, **4** and **5** as extracted from MP2/6-31G\* wavefunctions<sup>a</sup>

Atom	3a	3b	3c	4a	4b	4c	5
C1	0.00	0.08	0.12	–0.02	0.04	0.07	–0.05
C3	–0.1	–0.08	–0.09	–0.16	–0.17	–0.18	–0.14
C7	–0.03	–0.13	–0.11	–0.1	–0.18	–0.17	–0.18
X11	0.00	0.00	0.06	–0.24	–0.25	–0.16	–0.26
C6	–0.1	–0.1	–0.09	–0.16	–0.16	–0.18	–0.14
C10	–0.03	0.00	–0.11	–0.1	–0.09	–0.17	–0.18
X12	0.00	–0.01	0.06	–0.24	–0.24	–0.16	–0.26
H3	0.24	0.24	0.25	0.17	0.17	0.17	0.16
H7	0.26	0.23	0.24	0.19	0.17	0.17	0.17
H6	0.24	0.25	0.25	0.17	0.18	0.17	0.16
H10	0.26	0.27	0.24	0.19	0.19	0.17	0.17
H11	0.21	0.25	0.25	0.08	0.08	0.09	0.15
H12	0.21	0.27	0.25	0.08	0.09	0.09	0.15

<sup>a</sup> For numbering of atoms see Scheme 1. The position of the hydrogen atoms is indicated by the number of the corresponding heavy atom given in italics.

Finally, dication **3b** features two entirely different subunits, one of them being similar to the 7-norbornadienyl cage in **3c** and the other one closely resembling structure of the 7-norbornadienyl cation ring in **3a** (Table 2). The latter is also similar to the 7-norbornadienyl unit of cation **6** (Scheme 3). To highlight this close correspondence, we compare the C(1)–C(2) and C(1)–C(11)/C(2)–C(12) distances. In **3a** they amount 1.407 Å and 1.705 Å as compared to 1.418 Å and 1.695 Å in **6c**. Another feature that indicates close resemblance in bond character of these two structures is the similar size and direction of the pyramidalisation on C(1) and C(2), as indicated by out-of-plane bending angle  $\phi$  (–19.3° in **3b** vs. –16.2° in **6c** at the MP2 level).

We conclude this section by comparing the out-of plane angle potentials for the central double bond in structures **3a–3c**. This is of considerable interest, since structures **3b** and **3c** exhibit bending of the molecular framework opposite to that found in **3a**, or in the neutral *syn*-sesquinorbornene<sup>5a</sup> i.e. in both of these structures the C atoms, of the central double bond are pyramidalised in the *exo*-direction. The calculations were carried out by scanning the out-of-plane angle of the central double bond between –30° and +30°. All remaining geometrical parameters have been optimised at each point of scan using B3LYP method. The resulting potential curves, which are displayed in Fig. 2, demonstrate that out of plane bending in all three structures is rather flat, but less than that in the neutral sesquinorbornenes.<sup>5a</sup> This is substantiated by the calculation of the harmonic vibration frequencies of 115.3 cm<sup>–1</sup> and 139.7 cm<sup>–1</sup> and 161.1 cm<sup>–1</sup> (B3LYP values) for **3a**, **3b** and **3c**, respectively. The corresponding value for e.g. *syn*-sesquinorbornene is 135.7 cm<sup>–1</sup> at the same level of theory. It is noteworthy that harmonic vibration frequencies increase in moving from **3a** to **3c**, as intuitively expected. We also note that change in the direction of the out-of-plane bending in **3b** is energetically somewhat less costly than in **3c**. It should be, however, stressed that in both of these structures changing the sign of the angle  $\phi$  leads to disruption of the multicentre bond between cationic centre(s) and the central double bond. This is not surprising since the gain in stabilisation upon forming the C(11)–C(1)–C(2) bond in **3b** is obviously insufficient to compensate the increase in the charge–charge repulsion.

#### Structure and energetics of 4

The neutral structures **4a–4c**, which will be considered in this section, are isoelectronic with dications **3a–3c** but are not subject to the effect of charge repulsion. Consequently, the difference in their relative stabilities is expected to be attenuated

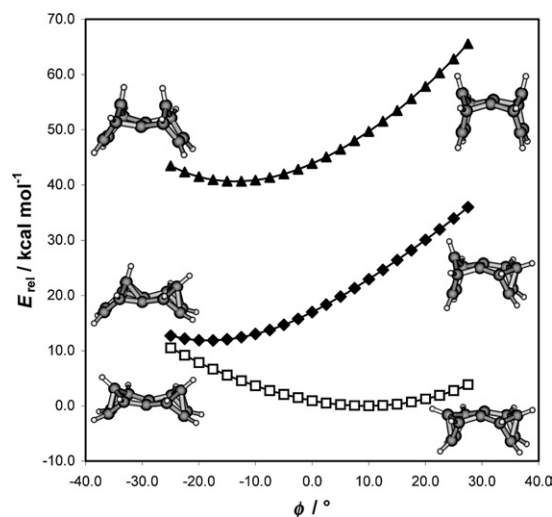


**Fig. 2** Out of plane bending potentials (B3LYP/6-31G\*) for **3a–3c**.

relative to the dication series, as indeed found (*vide infra*). Similarly, the activation energy for interconversion between structures between **4a** and **4b** and between **4b** and **4c** are significantly lower than for corresponding dications (Fig. 3) indicating that these processes would be more facile than in dication series.

The other major difference between systems **3a–3c** and **4a–4c** concerns stability ordering. Whereas in dications the structure **3a** is the most stable one, in 7,7'-diborasesquinorbornatrienes the form **4b** is energetically favoured. This is apparently consequence of energetically more favourable interaction of one of the BH bridges with the central double bond in structure **4b**. The structure **4c** is, likewise in the dication series, the highest in energy, in accordance with the conclusion that 4c/2e bonding in the *syn*-sesquinorbornene framework is energetically less favourable than the 3c/2e bonding.<sup>6</sup>

Perusal of the calculated bond distances and bond angles of structures **4a–4c** shows similar trend of changes as in the related dications **3a–3c** (Table 2). All three structures exhibit pronounced tilting of the BH bridges involved into 3c/2e (structures **4a** and **4b**) or 4c/2e (structure **4c**) bonding, with the former being more pronounced. For **4a** and **4b** these quantities are 80° and 79°, respectively, compared to 92.8° in **4c** (MP2). The same holds for nonbonded distances between the bridging groups and the corresponding double bond (Table 2). The calculated bond distances are also in good agreement with the calculated structure of 7-boranorbornadiene<sup>34</sup> and available X-ray data.<sup>35</sup> For instance, in the most stable structure **4b**, the C(1)–B(11)/C(2)–B(11) and C(9)–B(12)/C(10)–B(12) are 1.743 Å and 1.773 Å (at the MP2 level) compared to 1.759 Å in 7-boranorbornadiene at the same level of theory.<sup>36</sup> The agreement with the corresponding experimental value of 1.844 Å obtained by X-ray analysis of 7-phenylbora-1,2,3,4,5,6-hexamethylnorbornadiene is less satisfactory but is not surprising since the phenyl group at C(7) is known to lead to a considerable weakening of bis-homoaromatic interaction.<sup>4a,5b,35</sup> Similarly, the C(7)–C(8) and C(9)–C(10) distances in structure **4b**, 1.347 Å and 1.394 Å, respectively, are close to that of 7-boranorbornadiene (1.344 Å and 1.392 Å, respectively) and follow the trend encountered in the related dication **3b** (Table 2). The corresponding experimental values are 1.327 Å and 1.388 Å, respectively. Finally, it is interesting to note that the central double bond (1.398 Å) is longer than in *syn*-sesquinorbornatriene (1.360 Å, MP2) but is not as long as in the related dication **3b** (1.407 Å, Table 2).

It is noteworthy that the energy difference between structures **4a** and **4b** is practically identical to that found between the two energy minima, **7c** and **7p**, obtained for model molecule **7** shown in Scheme 4.

The same holds for geometry of the 7-boranorbornadiene fragments. More specifically, the calculated equivalent bond lengths are similar, differing by at most 0.011 Å (see Table 2 and Scheme 4). Similarly, bond angles differ by at most 0.4°. Another feature that indicates a close resemblance in bond character between monocation and dication structures is the

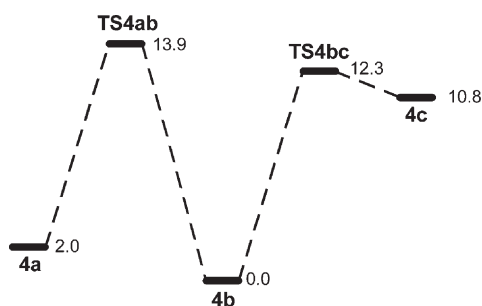
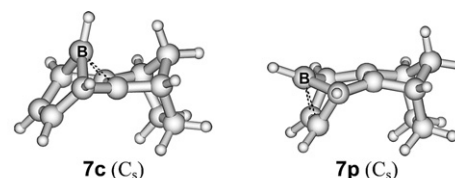


Fig. 3 Schematic energy diagram of the **4a–4c** system computed at the B3LYP level. Relative energies are given in kcal mol<sup>−1</sup>.



C(1)–C(2)	1.404 Å	1.360 Å
B(11)–C(12)	3.114 Å	4.603 Å
$\phi$	−9.0°	23.5°
$\alpha$	79.3°	152.5°
$\tau$	7.3°	−17.6°

Scheme 4 MP2 calculated structures and selected structural parameters of structures **7c** and **7p**. Letters **c** and **p** stand for the 3c/2e bonding with the central (**7c**) and the peripheral (**7p**) double bond. More complete compilation of the calculated bond distances and bond angles is given in Table S1 of the ESI†.

similar size and direction of the pyramidalisation of olefinic carbon atoms participating in the 3c/2e bond(s). The monocation **6c** has, for example, bonds emanating from the central bridge bent out of the plane in the *exo* direction by −16.2°, which is close to the **3b** value of −19.3° for equivalent bending. The other dihedral angles are also in the expected range and show no peculiarities.

#### Electronic structure and NMR chemical shifts of **3** and **4**

In order to gain additional insight into the nature of charge delocalization in **3** and **4** we carried out calculations of the formal atomic charges and the <sup>13</sup>C, as well as <sup>11</sup>B where appropriate, NMR chemical shifts for all of the considered species. For the sake of consistency with previous study on **1** and **2**,<sup>6</sup> the charge distribution was calculated using Löwdin orthogonalisation procedure, whereas the chemical shifts were calculated using GIAO approach. Moreover, previous experience for **1** and **2** and related compounds studied in ref. 6, has demonstrated that Löwdin charges, as well as the GIAO chemical shifts provide a reliable test for probing the nature of homoaromatic bonding in this family of compounds. The calculated charges are compiled in Table 3, while Table 4 lists the

Table 4 Comparison of calculated <sup>13</sup>C- and <sup>11</sup>B-NMR chemical shifts for **5**, **3** and **4**, as calculated by GIAO/6-311+G\*\* method at the B3LYP and MP2 geometries, the later being given within parentheses

Compound	Atom						
	C(1)	C(3)	C(7)	X(11)	C(6)	C(10)	X(12)
<b>5</b>	185.8 (191.7)	57.3 (56.1)	150.8 (153.0)	78.3 (77.4)	57.3 (56.1)	150.8 (153.0)	78.3 (77.4)
<b>3a</b>	148.9 (150.6)	62.8 (62.6)	125.3 (125.0)	48.2 (45.2)	62.8 (62.6)	125.3 (125.0)	48.2 (45.2)
<b>3b</b>	139.9 (139.0)	72.5 (73.1)	139.6 (141.4)	47.5 (43.9)	62.0 (61.6)	127.2 (127.4)	52.0 (49.2)
<b>3c</b>	140.8 (138.4)	70.1 (68.7)	145.2 (146.7)	136.1 (125.9)	70.1 (68.7)	145.2 (146.7)	136.1 (125.9)
<b>4a</b>	146.5 (148.8)	57.6 (58.2)	117.1 (116.6)	−66.5 (−84.0)	57.6 (58.2)	117.1 (116.6)	−66.5 (−84.0)
<b>4b</b>	133.6 (134.5)	59.9 (61.2)	137.7 (139.4)	−60.5 (−76.3)	56.3 (56.8)	119.0 (119.2)	−62.2 (−78.7)
<b>4c</b>	132.1 (132.9)	47.7 (46.8)	140.1 (141.7)	−37.7 (−55.0)	47.7 (46.8)	140.1 (141.7)	−37.7 (−55.0)
<b>8<sup>a</sup></b>	123.3 (122.7)	68.4 (68.3)	134.8 (136.3)	44.2 (40.9)			
<b>9<sup>a</sup></b>	117.1 (117.0)	61.3 (62.0)	133.1 (134.3)	−62.5 (−79.5)			

<sup>a</sup> in species **8** and **9** C(1) atom is involved in the 3c/2e bonding.

chemical shifts. The latter are calculated for the MP2 and B3LYP optimised geometries. Also included in Table 4 are relevant NMR parameters for reference molecules **5**, **8** and **9**. Analysis of the calculated chemical shifts reveals that the calculated  $^{13}\text{C}$  chemical shifts for the 7-norbornadienyl cage in structures **3a** and **3b** are very similar to the values calculated for the “free” 7-norbornadienyl cation (Table 4). For example, the carbon atom of the cationic centre in structures **3a** and **3b** is only 4.2 ppm and 3.2 ppm, respectively, less shielded than that in the 7-norbornadienyl cation (for MP2 geometry). These results are fully compatible with the conclusion that these species exhibit similar non-classical bonding. It is also worth mentioning that all these ions have similar charge distribution over the atoms involved into 3c/2e bonding with the charge at the cationic centre (Table 3) within Löwdin’s partitioning scheme, being close or equal to zero meaning that the positive charge is strongly delocalised. In this regard it is also of interest to compare carbon chemical shifts and charge distribution between dications **3a** and **3b** and the 4c/2e structure, **3c**. The calculated chemical shift of the cationic centres in **3c** is 136.1 ppm, which implies  $\sim 90$  ppm downfield shift from the  $\delta^{13}\text{C}$  value for that atom in structures **3a** and **3b**. The observed trend is in accordance with the partial positive charge of this carbon in the latter case (Table 3). This in turn, shows that the effectiveness of the charge depletion from the cationic centre in the 4c/2e dication is significantly reduced relative to the dications with the 3c/2e bonding, in accordance with discussion based on structural arguments. It is also of interest to note that the olefinic C(1) and C(2) atoms in all dicationic structures are shielded by  $\sim 30$  ppm relative to the neutral molecule **5**. In contrast, the  $^{13}\text{C}$  resonance of the bridgehead carbon atoms move to the higher field than in **5** (see Table 4).

The calculated  $^{11}\text{B}$  chemical shifts in **4a–4b** are negative, in line with  $^{11}\text{B}$  chemical shift calculated for 7-boronorbornadiene ( $-62.5$  ppm and  $-79.5$  ppm at B3LYP and MP2 geometries, respectively), and the available experimental data. Apparently, shielding of the boron atoms in these species is consistent with the non-classical nature of these compounds. It should be also pointed out that the  $^{11}\text{B}$  chemical shifts in structure **4c** are less shielded than in its 3c/2e counterparts, **4a** and **4b**, suggesting again that the interaction within the BCC triangle is stronger in the latter structures. Analysis of the calculated charges for structures **4a–4c** fully supports this conclusion. The changes in the  $^{13}\text{C}$  chemical shifts follow the trends found for dications and show no peculiarities.

We shall conclude this section by comparing electronic structure of the most stable form of **4** with that of the *syn*-sesquiorbornatriene (**5**). This is of considerable interest since our calculations reveal that replacement of the  $\text{CH}_2$  bridges in the latter has pronounced effect on the size and direction of the pyramidalisation of olefinic carbon atoms at the central and one of the peripheral double bonds (Table 2). This in turn leads to the change in the shape and energy ordering of the frontier MOs as indicated in Fig. 4.<sup>37</sup> For instance, in the hydrocarbon **5** the HOMO is mainly localized at the central bridge, whereas the HOMO of **4b** has the largest coefficients at the peripheral double bond which doesn’t participate in the 3c/2e bonding. The latter MO is lower in energy by 0.49 eV than HOMO in **5**. Similarly, the LUMO in **5** has the largest coefficients at the central double bond, while the LUMO of **4** is mainly localized over the atoms involved in 3c/2e bond. Consequently, we expect profound difference in reactions controlled by orbital symmetry.<sup>38</sup>

An interesting question related to this issue concerns potential difference in  $\pi$ -facial stereoselectivity in addition reactions to **1** and **2**. Namely, in contrast to **1** molecule **2** exhibits out-of-plane bending of the molecular framework in the *exo,exo* direction.<sup>6</sup> This suggests that replacement of the  $\text{CH}_2$  bridges with the BH groups might, *inter alia*, lead to preferential addition of some reagents from the opposite site than in **1**; *i.e.* from

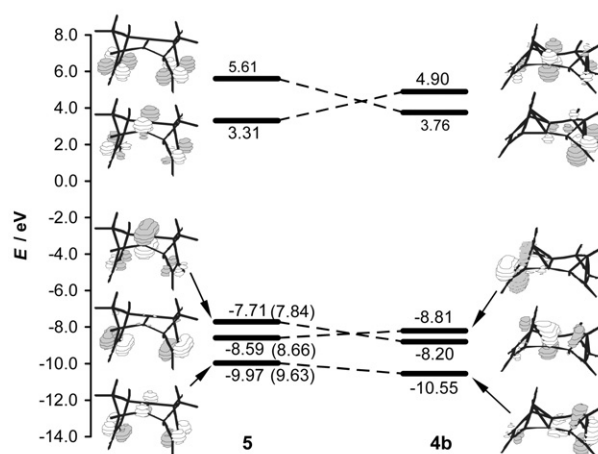


Fig. 4 Comparison of the highest occupied and the lowest unoccupied MOs in **5** and **4b** as calculated by HF/6-31G\*//MP2/6-31G\*. Experimentally measured vertical ionisation energies for **5** are given in parentheses.<sup>30</sup>

the *endo* face of the molecule. The reversal of  $\pi$ -facial stereoselectivity in cycloaddition reactions of *syn*-sesquiorbornene has been hitherto discussed and experimentally observed<sup>39,40</sup> only upon irradiation and was attributed to the electronic and steric factors inherent to the *exo*-bent geometry of the triplet state.<sup>41,42</sup>

## Conclusions

In this study structure of dication **3** derived by replacement of the  $\text{CH}_2$  bridges in *syn*-sesquiorbornene (**5**) with the  $^+\text{CH}$  groups and its isoelectronic boron analogue **4** were investigated using *ab initio* MP2/6-31G\* and density functional B3LYP/6-31G\* methods. For both species three energy minima were located on the PES, all of them exhibiting strong bis-homoaromatic interaction of the electron deficient bridges with either central or peripheral double bond(s). This is reflected in the characteristic bending of the  $^+\text{CH}$  and BH bridges, respectively, toward the interacting double bond and the lengthening of the latter. It was also shown that the most stable structure of dication **3** differs from that of **4**. While in **3** both  $^+\text{CH}$  groups interact with the peripheral double bonds, in **4** one of the BH groups interacts with the central and the other with the peripheral double bond. This was attributed to the prevailing importance of the electrostatic interaction in the dication. Another salient difference between the two species concerns a direction of out-of-plane bending of the molecular framework from the hinge-like in **3** to the *exo,exo* fashion in **4**. Consequences of the latter on reactivity of **4** and its tetrahydro analogue **2** were discussed. In particular it was proposed that replacement of the  $\text{CH}_2$  groups in *syn*-sesquiorbornene moiety with the BH bridges might lead to reversal of  $\pi$ -facial stereoselectivity in cycloaddition reactions. In other words we propose that **2**, unlike **1** might undergo cycloadditions from the *endo* face of the molecule.

## Acknowledgements

Financial support by the Ministry of Science and Technology of Croatia (Project No. 0098056) is gratefully acknowledged.

## References

- For a pertinent reviews see *e.g.* (a) S. Winstein in *Carbonium Ions*, eds. G. A. Olah, P. v. R. Schleyer, John Wiley, New York, 1972, vol. III; (b) P. Vogel, *Carbocation Chemistry*, Elsevier,



- Amsterdam, 1985. (c) D. Lenoir and H.-U. Siehl in *Houben-Weyl*, ed. M. Honach, Thieme Verlag, Stuttgart, 1990, Vol. 19c; (d) R. V. Williams and H. A. Kurtz, *Adv. Phys. Org. Chem.*, 1994, **29**, 273; (e) R. V. Williams, *Chem. Rev.*, 2001, **101**, 1185.
- 2 (a) S. Winstein, M. Shatavsky, C. Norton and R. B. Woodward, *J. Am. Chem. Soc.*, 1955, **77**, 4183; (b) W. G. Woods, R. A. Carboni and J. D. Roberts, *J. Am. Chem. Soc.*, 1956, **78**, 5653; (c) S. Winstein, *J. Am. Chem. Soc.*, 1960, **82**, 2084; (d) P. R. Story and M. Saunders, *J. Am. Chem. Soc.*, 1962, **84**, 4876; (e) M. Brookhart, R. K. Lustgarten and S. Winstein, *J. Am. Chem. Soc.*, 1967, **89**, 6352.
  - 3 (a) G. A. Olah and G. Liang, *J. Am. Chem. Soc.*, 1975, **97**, 6803; (b) G. A. Olah, A. L. Berrier, M. Arvanaghi and G. K. Surya-Prakash, *J. Am. Chem. Soc.*, 1981, **103**, 1122.
  - 4 (a) T. Laube, *J. Am. Chem. Soc.*, 1989, **111**, 9224; (b) T. Laube and C. Lohse, *J. Am. Chem. Soc.*, 1994, **116**, 9001; (c) T. Laube, *Acc. Chem. Res.*, 1995, **28**, 399 and references therein; (d) W. J. Evans, K. J. Forrestal and J. W. Ziller, *J. Am. Chem. Soc.*, 1995, **117**, 12635.
  - 5 (a) M. C. Holthausen and W. Koch, *J. Phys. Chem.*, 1993, **97**, 10021; (b) M. Bremer, K. Schötz, P. v. R. Schleyer, U. Fleischer, M. Schindler, W. Kutzelnigg, W. Koch and P. Pulay, *Angew. Chem., Int. Ed. Engl.*, 1989, **28**, 1042; (c) R. Gleiter and J. Spanget-Larsen, *Tetrahedron Lett.*, 1982, **23**, 927; (d) G. Wipff and K. Morokuma, *Chem. Phys. Lett.*, 1980, **74**, 400; (e) G. Wipff and K. Morokuma, *Tetrahedron Lett.*, 1980, **21**, 4446; (f) N. G. Rondan, M. N. Paddon-Row, P. Caramella and K. N. Houk, *J. Am. Chem. Soc.*, 1981, **103**, 2436; (g) S. Yoneda, Z. Yoshida and S. Winstein, *Tetrahedron*, 1972, **28**, 1395.
  - 6 M. Eckert-Maksić, I. Antol, D. Margetić and Z. Glasovac, *J. Chem. Soc., Perkin Trans.*, 2002, **2**, 2057.
  - 7 See e.g. *Stereochemistry and Reactivity of Systems Containing  $\pi$ -Electrons*, ed. W. H. Watson, VCH International, Deerfield Beach, Florida, 1983.
  - 8 (a) W. H. Watson, J. Galloy, P. D. Bartlett and A. A. M. Roof, *J. Am. Chem. Soc.*, 1981, **103**, 2022; (b) O. Ermer, *Tetrahedron*, 1974, **30**, 3103; (c) J.-P. Hagenbuch, P. Vogel, A. A. Pinkerton and D. Schwarzenbach, *Helv. Chim. Acta*, 1981, **64**, 1818; (d) L. A. Paquette, T. M. Kravetz and L. -Y. Hsu, *J. Am. Chem. Soc.*, 1985, **107**, 6598.
  - 9 IUPAC name: tetracyclo[6.2.1.1<sup>3,6</sup>.0<sup>2,7</sup>]dodec-2(7),4,9-triene.
  - 10 P. C. Hariharan and J. A. Pople, *Theor. Chim. Acta*, 1973, **28**, 213.
  - 11 (a) A. D. Becke, *J. Chem. Phys.*, 1993, **98**, 5648; (b) C. Lee, W. Yang and R. G. Parr, *Phys. Rev. B*, 1988, **37**, 785; (c) B. Michlich, A. Savin, H. Stoll and H. Preuss, *Chem. Phys. Lett.*, 1989, **157**, 200.
  - 12 (a) J. A. Pople, J. S. Binkley and R. Seeger, *Int. J. Quantum Chem. Symp.*, 1976, **10**, 1; (b) R. Krishnan and J. A. Pople, *Int. J. Quantum Chem.*, 1978, **14**, 91.
  - 13 (a) I. Antol, M. Eckert-Maksić, D. Margetić, Z. B. Maksić, K. Kowski and P. Rademacher, *Eur. J. Org. Chem.*, 1998, 1403; (b) D. Margetić, R. N. Warrener, M. Eckert-Maksić, I. Antol and Z. Glasovac, *Theor. Chem. Acc.*, 2003, **109**, 182.
  - 14 (a) M. C. Holthausen and W. Koch, *J. Phys. Chem.*, 1993, **97**, 10021; (b) R. V. Williams, W. D. Edwards, V. R. Gadgil, M. E. Colvin, E. T. Seidl, D. v. der Helm and M. B. Hossain, *J. Org. Chem.*, 1998, **63**, 5268; (c) A. G. Griesbeck, T. Deufel, G. Hohlneicher, R. Rebentisch and J. Steinwascher, *Eur. J. Org. Chem.*, 1998, 1759; (d) H. Can, D. Zahn, M. Balci and M. Brickmann, *Eur. J. Org. Chem.*, 2003, **6**, 1111; (e) D. Margetić, R. V. Williams and R. N. Warrener, *J. Org. Chem.*, 2003, **68**, 9186.
  - 15 See e.g. W. J. Hehre, L. Radom, P. v. R. Schleyer and J. A. Pople, *Ab Initio Molecular Orbital Theory*, Wiley, New York, 1986.
  - 16 A. P. Scott and L. Radon, *J. Phys. Chem.*, 1996, **100**, 16 502.
  - 17 C. Gonzalez and H. B. Schlegel, *J. Phys. Chem.*, 1990, **94**, 5523.
  - 18 (a) K. Wolinski, J. F. Hinton and P. Pulay, *J. Am. Chem. Soc.*, 1990, **112**, 8251; (b) R. Ditchfield, *Mol. Phys.*, 1974, **27**, 789.
  - 19 P.-O. Löwdin, *J. Chem. Phys.*, 1950, **18**, 365.
  - 20 MOLDEN4.0, G. Schaftenaar and J. H. Noordik, *J. Comput.-Aided. Mol. Design*, 2000, **14**, 123.
  - 21 M. J. Frisch, G. W. Trucks, H. B. Schlegel, G. E. Scuseria, M. A. Robb, J. R. Cheeseman, V. G. Zakrzewski, J. A. Montgomery, Jr., R. E. Stratmann, J. C. Burant, S. Dapprich, J. M. Millam, A. D. Daniels, K. N. Kudin, M. C. Strain, O. Farkas, J. Tomasi, V. Barone, M. Cossi, R. Cammi, B. Mennucci, C. Pomelli, C. Adamo, S. Clifford, J. Ochterski, G. A. Petersson, P. Y. Ayala, Q. Cui, K. Morokuma, D. K. Malick, A. D. Rabuck, K. Raghavachari, J. B. Foresman, J. Cioslowski, J. V. Ortiz, B. B. Stefanov, G. Liu, A. Liashenko, P. Piskorz, I. Komaromi, R. Gomperts, R. L. Martin, D. J. Fox, T. Keith, M. A. Al-Laham, C. Y. Peng, A. Nanayakkara, C. Gonzalez, M. Challacombe, P. M. W. Gill, B. G. Johnson, W. Chen, M. W. Wong, J. L. Andres, M. Head-Gordon, E. S. Replogle and J. A. Pople, *GAUSSIAN 98 (Revision A.7)*, Gaussian, Inc., Pittsburgh, PA, 1998.
  - 22 GAMESS M. W. Schmidt, K. K. Baldridge, J. A. Boatz, S. T. Elbert, M. S. Gordon, J. H. Jensen, S. Koseki, N. Matsunaga, K. A. Nguyen, S. J. Su, T. L. Windus, M. Dupuis and J. A. Montgomery, *J. Comp. Chem.*, 1993, **14**, 1347.
  - 23 In this paper the out-of-plane deformation of a double bond will be described using the flap or hinge angle  $\phi$ :  $^{24} 180^\circ - \gamma$ , where  $\gamma$  corresponds to the dihedral angle between C(3)–C(2)–C(1)–C(4) and C(6)–C(2)–C(1)–C(5) planes. Similarly,  $\tau_1$ ,  $\tau_2$ ,  $\alpha$ ,  $\alpha_1$ ,  $\beta$  and  $\beta_1$  are defined as the angles between the following planes:  $\tau_1$ : C(4)–C(8)–C(7)–C(3) and H–C(8)–C(7)–H;  $\tau_2$ : C(6)–C(10)–C(9)–C(5) and H–C(10)–C(9)–H;  $\alpha$ : C(3)–X(11)–C(4) and C(3)–C(2)–C(1)–C(4);  $\beta$ : C(3)–X(11)–C(4) and C(3)–C(7)–C(8)–C(4);  $\alpha_1$ : C(6)–X(12)–C(5) and C(6)–C(2)–C(1)–C(5) and  $\beta_1$ : C(6)–X(12)–C(5) and C(6)–C(10)–C(9)–C(5). For alternative descriptions of the pyramidalisation angles see refs. 25–27.
  - 24 O. Ermer and C.-D. Bödecker, *Helv. Chim. Acta*, 1983, 943.
  - 25 T. W. Borden, *Chem. Rev.*, 1989, **89**, 1095.
  - 26 S. F. Nelsen, T. B. Frigo and Y. Kim, *J. Am. Chem. Soc.*, 1989, **111**, 5387.
  - 27 R. C. Haddon, *J. Am. Chem. Soc.*, 1990, **112**, 3385.
  - 28 The name sandwiched bis-homoaromatic was coined by Olah and coworkers<sup>29</sup> to describe bonding in *anti*-tricyclo[4.2.1.1<sup>2,5</sup>]deca-3,7-diene-9,10-diyl dication.
  - 29 G. K. S. Prakash, G. Rasul, A. K. Yudin and G. A. Olah, *Gazz. Chim. Ital.*, 1996, **126**, 1.
  - 30 H. Kunzer, E. Litterst, R. Gleiter and L. A. Paquette, *J. Org. Chem.*, 1987, **52**, 4740.
  - 31 E. Heilbronner and H. Bock, *Das HMO Modell und Seine Anwendung*, Verlag Chemie, Weinheim, 1986.
  - 32 Qualitatively, similar results are also obtained by Mulliken as well as by NPA analysis. Both are available on request from the author.
  - 33 (a) J. E. Carpenter and F. Weinhold, *J. Mol. Struct. Theochem*, 1988, **169**, 41; (b) J. P. Foster and F. Weinhold, *J. Am. Chem. Soc.*, 1980, **102**, 7211; (c) A. E. Reed and F. Weinhold, *J. Chem. Phys.*, 1983, **78**, 4066; (d) A. E. Reed, R. B. Weinstock and F. Weinhold, *J. Chem. Phys.*, 1985, **83**, 735; (e) A. E. Reed, L. A. Curtiss and F. Weinhold, *Chem. Rev.*, 1988, **88**, 899.
  - 34 (a) J. M. Schulman, R. L. Disch, P. v. R. Schleyer, M. Bühl, M. Bremer and W. Koch, *J. Am. Chem. Soc.*, 1992, **114**, 7897; (b) R. L. Disch, M. L. Sabio and J. M. Schulman, *Tetrahedron Lett.*, 1983, **24**, 1863.
  - 35 (a) P. J. Fagan, E. G. Burns and J. C. Calabrese, *J. Am. Chem. Soc.*, 1988, **110**, 2979; (b) P. J. Fagan, W. A. Nugent and J. C. Calabrese, *J. Am. Chem. Soc.*, 1994, **116**, 1880.
  - 36 Present work, see also ref. 34a.
  - 37 It should be noted that the calculated IE of **5** are by ~2 eV lower than the experimental IEs.<sup>30</sup> However, there is a close parallelism between the calculated energy differences involving the first three MOs and those of the measured IE.
  - 38 K. Fukui, *Theory of Orientation and Stereoselection*, Springer Verlag, Berlin-Heidelberg-New York, 1975 and references therein.
  - 39 P. D. Bartlett, A. J. Blakeney, G. L. Combs, J. Galloy, A. A. M. Roof, R. Subramanyam, W. H. Watson, W. J. Winter and C. Wu in *Stereochemistry and Reactivity of Systems Containing  $\pi$ -Electrons*, ed. W. H. Watson, Verlag Chemie International, Derfield Beach FL, 1983, p. 75 and references cited therein.
  - 40 Bartlett, A. A. M. Roof and W. J. Winther, *J. Am. Chem. Soc.*, 1981, **103**, 6520.
  - 41 K. N. Houk, N. G. Radon, F. K. Brown, W. L. Jorgensen, J. D. Madura and D. C. Spelemeyer, *J. Am. Chem. Soc.*, 1983, **105**, 5980.
  - 42 J. Spanget-Larsen and R. Gleiter, *Tetrahedron*, 1983, **39**, 3345.